(Received 25 January 2025, Accepted 16 March 2025, Scheduled 24 March 2025)

Two Methods for Convergence Determination of EMC Uncertainty Analysis Based on Variance and Failure Rate

Jinjun Bai*, Shenghang Huo, Huiyan Hou, Xingfeng Cao, and Yilai Ren

College of Marine Electrical Engineering, Dalian Maritime University, Dalian 116026, China

ABSTRACT: The uncertainty analysis method based on surrogate models is a current research topic in electromagnetic compatibility (EMC) simulation. However, the research on its convergence determination remains underdeveloped. Based on the multi-surrogate model integration technique, this paper proposes two convergence determination methods: one based on variance and the other on failure rate. Researchers can select the appropriate convergence determination method based on specific application requirements, ultimately identifying the optimal number of sample points to ensure the accuracy and efficiency in EMC uncertainty analysis.

1. INTRODUCTION

Uncertainties in system parameters due to fabrication tolerances and device characteristics can severely affect the system response. Uncertainty analysis has been introduced into EMC simulation in order to ensure an accurate evaluation of system performance and to avoid costly redesigns [1]. The computationally expensive Monte Carlo Method (MCM) was widely used in early EMC uncertainty analysis for its high accuracy [2]. However, MCM poses significant challenges regarding computational resources and simulation time, particularly in large-scale and highly complex EMC simulations [3].

In recent years, with the development of machine learning, surrogate models have been widely used in EMC uncertainty analysis for their high efficiency and low cost [4]. Lagouanelle et al. [5] utilized two surrogate models — Kriging and Polynomial Chaos Expansion (PCE) — to analyze the uncertainty of human electromagnetic exposure in an electric vehicle Wireless Power Transfer (WPT) system. Wang et al. [6] examined the Specific Absorption Rate (SAR) uncertainty in the electric vehicle WPT system for specific human organs using a modified PCE. Trinchero et al. [7] explored the use of Support Vector Regression (SVR) and Least Squares Support Vector Regression (LSSVR) for uncertainty analysis in complex EMC systems with high-dimensional parameter spaces.

The surrogate model-based uncertainty analysis method addresses the challenges of costly and inefficient MCM computations [8]. However, determining the optimal number of sample points remains a critical issue: too few sample points result in inaccurate uncertainty analysis, with too many waste computational resources. Accurately determining the convergence of surrogate-based modeling for EMC uncertainty analysis is a critical issue that must be addressed. In 2021, Bai et al. [9] introduced a Mean Equivalent Area Method (MEAM)-based convergence determination method for the Stochastic Reduced Order Model (SROM). However, its primary limitation lies in its poor adaptability, making it unsuitable for determining the convergence of other surrogate models. In 2024, Hu et al. [10] enhanced the MEAM method to enable the convergence determination of surrogate models. However, this approach relies on user experience to determine the required number of sampling points, limiting its applicability.

To address the gap in research on the convergence determination of uncertainty analysis using surrogate models, this paper proposes two methods based on variance and failure rate. The two convergence determination methods are applied to three widely used surrogate models: PCE, Kriging, and SVR. The two convergence determination methods are proposed from the perspectives of overall accuracy and system failure in EMC uncertainty analysis, offering a multifaceted reference for selecting the optimal number of sample points for surrogate models.

The paper is organized as follows, Section 2 provides an overview of uncertainty analysis and briefly introduces the principles of three surrogate models: PCE, Kriging, and SVR. The principles and steps of the two convergence determination methods based on variance and failure rates are presented in Section 3. In Section 4, the proposed convergence determination methods are applied to the three classical surrogate models for the metal box shielding effectiveness example. Section 5 summarizes the paper.

2. UNCERTAINTY ANALYSIS METHODS BASED ON SURROGATE MODELING

Uncertainty analysis methods typically use a random variable model in vector form to characterize uncertainty factors, as shown below:

$$\xi = \{\xi_1, \xi_2, \ldots, \xi_j, \ldots, \xi_m\} \tag{1}$$

where ξ_j is a random variable, ξ a vector of random variables, and m the number of random variables.

* Corresponding author: Jinjun Bai (baijinjun@dlmu.edu.cn).

The MCM is based on the weak law of large numbers, utilizing a large number of sample points $\mathbf{S}_1 = [\mathbf{X}_1, \mathbf{X}_2, \ldots, \mathbf{X}_n]$ to represent the random variable vector ξ. In essence, it considers almost all sample points within the sample space, where the number of sampling points is assumed to be n, and each sampling point $\mathbf{X}_i$ is m-dimensional vector data as follows:

$$\mathbf{X}_i = \{X_i(1), X_i(2), \ldots, X_i(j), \ldots, X_i(m)\} \tag{2}$$

where $X_i(j)$ is a definite constant value, which corresponds to ξ_j in Equation (1).

To perform uncertainty analysis using the surrogate model, the first step involves sampling the space (in this paper, the Latin hypercube sampling method is employed) to obtain the sampling points $\mathbf{S}_2 = [\mathbf{x}_1, \mathbf{x}_2, \ldots, \mathbf{x}_N]$. Next, a deterministic EMC simulation is conducted on $\mathbf{S}_2$ to generate the training set $\{\mathbf{x}_i, y_i\}_{i=1}^N$. The surrogate model $\hat{y} = \mathrm{M}(\mathbf{x})$ is constructed based on the training set. Finally, the response values on a large number of sampling points $\mathbf{S}_1$ are predicted based on the surrogate model to obtain the uncertainty analysis results.

This section describes the three surrogate models applied in this paper: PCE, Kriging, and SVR.

2.1. PCE

The expansion of PCE is shown in Equation (3):

$$\hat{y} = \mathrm{M_{PCE}}(\mathbf{x}) = \sum_{\mathrm{i=0}}^{\mathrm{P-1}} \alpha_\mathrm{i}\varphi_\mathrm{i}(\mathbf{x}) \tag{3}$$

where $\varphi_i(\mathbf{x})$ is an orthogonal polynomial that depends on the type of distribution of the random variable (the random variable in this example obeys a uniform distribution, so $\varphi_i(\mathbf{x})$ is a Legendre polynomial). α_i is the deterministic expansion coefficient of the solution to be solved, which can be solved from the training set $\{\mathbf{x}_i, y_i\}_{i=1}^N$ by regression techniques [6].

The number of terms P (The number of chaos polynomials in Equation (3)) of the expansion is shown in Equation (4):

$$P = \frac{(m+q)!}{m!q!} \tag{4}$$

where m is the number of input random variables, and q is the order of the expansion.

2.2. Kriging

As an interpolation model, Kriging generates interpolated results by linearly weighting the EMC simulation outputs $\mathbf{y} = [y_1, y_2, \ldots, y_N]^\mathrm{T}$ at the sample points $\mathbf{S}_2$.

$$\hat{y} = \mathrm{M_{Kriging}}(\mathbf{x}) = \sum_{\mathrm{i=1}}^{\mathrm{N}} \mathrm{w_i y_i} \tag{5}$$

where $\mathbf{w} = [w_1, w_2 \ldots w_N]^\mathrm{T}$ is the weighting coefficient, and the response value of any point in the sampling space can be obtained by giving the value of the weighting coefficient $\mathbf{w}$.

From the conclusions drawn in the literature [11], the Kriging model can be expressed as:

$$\mathrm{M_{Kriging}}(\mathbf{x}) = \beta_0 + \mathbf{r}^\mathrm{T}(\mathbf{x})\mathbf{R}^{-1}(\mathbf{y} - \beta_0\mathbf{F}) \tag{6}$$

where $\beta_0 = (\mathbf{F}^\mathrm{T}\mathbf{R}^{-1}\mathbf{F})^{-1}\mathbf{F}^\mathrm{T}\mathbf{R}^{-1}\mathbf{y}$, $\mathbf{F} = \begin{bmatrix} 1, & 1, & \ldots, & 1 \end{bmatrix}^\mathrm{T}$, $\mathbf{R} = \begin{bmatrix} R(\mathbf{x}_1, \mathbf{x}_1) & \cdots & R(\mathbf{x}_1, \mathbf{x}_N) \\ \vdots & & \vdots \\ R(\mathbf{x}_N, \mathbf{x}_1) & \cdots & R(\mathbf{x}_N, \mathbf{x}_N) \end{bmatrix}$, and $\mathbf{r} = \begin{bmatrix} R(\mathbf{x}_1, \mathbf{x}) \\ \vdots \\ R(\mathbf{x}_N, \mathbf{x}) \end{bmatrix}$. Let $\mathbf{V}_{krig} = \mathbf{R}^{-1}(\mathbf{y} - \beta_0\mathbf{F})$, then both β_0 and $\mathbf{V}_{krig}$ are related only to known sample points.

2.3. SVR

SVR aims to learn the functional relationship between the inputs and outputs of the training set $\{\mathbf{x}_i, y_i\}_{i=1}^N$. The nonlinear SVR is expressed as follows:

$$\hat{y} = \mathrm{M_{SVR}}(\mathbf{x}) = \langle \mu, \phi(\mathbf{x}) \rangle + \mathrm{b} \tag{7}$$

where the nonlinear mapping $\phi(\cdot)$ maps the m-dimensional input space to the high-dimensional feature space. μ is a vector of nonlinear regression coefficients, and b is an offset parameter.

The SVR model is obtained from [7] as follows:

$$\mathrm{M_{SVR}}(\mathbf{x}) = \sum_{\mathrm{i=1}}^{\mathrm{N}} (\lambda_\mathrm{i} - \lambda_\mathrm{i}^*)\mathrm{K}(\mathbf{x}_\mathrm{i}, \mathbf{x}) + \mathrm{b} \tag{8}$$

where λ_i and λ_i^* are Lagrange multipliers, and $K(\mathbf{x}_i, \mathbf{x})$ is the kernel function ($K(\mathbf{x}_i, \mathbf{x}_j) = \phi(\mathbf{x}_i) \cdot \phi(\mathbf{x}_j)$).

3. TWO CONVERGENCE DETERMINATION METHODS BASED ON VARIANCE AND FAILURE RATE

For the uncertainty analysis of surrogate-based models, this paper proposes two convergence determination methods: variance-based convergence and failurerate-based convergence.

3.1. Convergence Determination Based on Variance

Variance evaluates the reliability of uncertainty analysis results from a holistic perspective, quantifying the degree of fluctuation in the surrogate model's predictions. The variance of the response values predicted by the surrogate model is given below.

$$\hat{\sigma}^2 = \frac{1}{n-1}\sum_{i=1}^{n}(Y_i - \bar{Y})^2 \tag{9}$$

where Y_i is the response value of the surrogate model for each sample in a large number of sampling points $\mathbf{S}_1$; $\bar{Y}$ is the mean of the predicted response values; and n is the number of sample points for $\mathbf{S}_1$.

The variance-based convergence determination proposed in this paper compares the surrogate model variance $\hat{\sigma}^2$ with the reference variance $\bar{\sigma}^2$ to determine whether the current number N of training sample points $\mathbf{S}_2$ satisfies the convergence condition. In the study of [12] the variance of the MCM results is used as the reference variance, and this method ensures the

Algorithm 1

Selection of initial training sample points $\mathbf{S}_2$ based on LHS
EMC Simulation $y_i = \mathrm{EMC}[\mathbf{x}_i]$
The training set $\{\mathbf{x}_i, y_i\}_{i=1}^{N}$ is obtained
Constructing surrogate models $\hat{y} = \mathrm{M}(\mathbf{x})$
Surrogate model variance $\hat{\sigma}^2$
Calculation of tolerance $\psi_v = \left|\hat{\sigma}^2 - \bar{\sigma}^2\right|$
if $(\psi_v > \tilde{\psi})$ then
  $N = N + d$
  Go to Step 2
else
  //Checking for convergence
  for $(k = 1 : 3)$ do
    $N = N + k \times d$
    Implementation of steps 2–6
    if $(\psi_v > \tilde{\psi})$ then
      Go to Step 2
    end if
  end for
end if
Converged surrogate models are output

Algorithm 2

Selection of initial training sample points $\mathbf{S}_2$ based on LHS
EMC Simulation $y_i = \mathrm{EMC}[\mathbf{x}_i]$
The training set $\{\mathbf{x}_i, y_i\}_{i=1}^{N}$ is obtained
Constructing surrogate models $\hat{y} = \mathrm{M}(\mathbf{x})$
Failure rate $\hat{P}_f$
Calculation of tolerance $\psi_f = \left|\hat{P}_f - \bar{P}_f\right|$
if $(\psi_f > \tilde{\psi}_f)$ then
  $N = N + d$
  Go to Step 2
else
  //Checking for convergence
  for $(k = 1 : 3)$ do
    $N = N + k \times d$
    Implementation of steps 2–6
    if $(\psi_f > \tilde{\psi}_f)$ then
      Go to Step 2
    end if
  end for
end if
Converged surrogate models are output

accuracy of the convergence determination, but sacrifices the computational efficiency, and even cannot be realized in complex engineering. The reference variance $\bar{\sigma}^2$ chosen in this paper is the mean of the variance of the three surrogate models: PCE, Kriging, and SVR. The integration of multiple surrogate models not only reduces the computational cost to a great extent, but also reduces the overfitting or underfitting problems that may occur in a single model, thus improving the stability of the overall prediction [13]. PCE is well suited for the global approximation of smooth response functions. The precise interpolation capability of Kriging enables it to account for local variations. SVR employs a kernel function to map data into a high-dimensional space, enhancing its robustness in nonlinear regions. Integrating these three surrogate models provides a more comprehensive representation of the response feature space, effectively addressing the adaptability limitations of traditional single-model approaches. The variance tolerance, defined in Equation (10), serves as a convergence indicator.

$$\psi_v = \left|\hat{\sigma}^2 - \bar{\sigma}^2\right| \tag{10}$$

Algorithm 1 outlines the procedure for variance-based convergence determination. First, the initial training sample points $\mathbf{S}_2$ are selected using Latin Hypercube Sampling (LHS). A deterministic EMC simulation is conducted on $\mathbf{S}_2$ to generate the training set $\{\mathbf{x}_i, y_i\}_{i=1}^{N}$. Next, surrogate models are constructed using the training set. The surrogate models are then applied to predict the response values Y_i at a large number of sampling points $\mathbf{S}_1$, and the variance of the surrogate model $\hat{\sigma}^2$ is calculated. Finally, the tolerance ψ_v between the surrogate model variance $\hat{\sigma}^2$ and reference variance $\bar{\sigma}^2$ is calculated. If the tolerance ψ_v exceeds the standard tolerance $\tilde{\psi}$ (defined based on actual requirements and set as $\tilde{\psi} = 5\% \times \bar{\sigma}^2$ in this paper), the number N of training sample points is increased incrementally by the step size d (d can be adjusted based on the specific needs of different cases or designers). When the tolerance ψ_v is less than or equal to the standard tolerance $\tilde{\psi}$, the tolerance ψ_v is incrementally checked over three step sizes: $N = N + d$, $N = N + 2d$, and $N = N + 3d$. If the tolerance ψ_v remains less than or equal to the standard tolerance $\tilde{\psi}$ in all three step sizes, convergence is confirmed.

3.2. Convergence Determination Based on Failure Rate

Failure rates can be used to assess the reliability of uncertainty analysis results in the perspective of system failure [14]. Let $R(\mathbf{x})$ denote the performance requirement of interest, and $\boldsymbol{x}$ is the random variable input to the system. If the performance satisfies the requirement, $R(\mathbf{x}) = 1$; if not, $R(\mathbf{x}) = 0$, indicating system failure.

The failure domain refers to the portion of the EMC uncertainty output where the system fails, i.e., the region where $R(\mathbf{x}) = 0$, denoted as $F = \{\mathbf{x} : R(\mathbf{x}) = 0\}$. The failure rate is defined as the proportion of the entire sample space occupied by points within the failure domain. In this paper, the failure rate is expressed using the probability density function (PDF), as shown in Equation (11).

$$\hat{P}_f = \int_F p(\varepsilon) d\varepsilon \tag{11}$$

where $p(\varepsilon)$ is the probability density function.

Convergence determination based on the failure rate involves comparing the failure rate $\hat{P}_f$ of the predicted response from the surrogate model with the reference failure rate $\bar{P}_f$ to assess whether the current number N of training sample points $\mathbf{S}_2$ meets the convergence condition. The reference failure rate $\bar{P}_f$ is the average of the failure rates from the three surrogate models. Combining the failure rates of multiple surrogate models

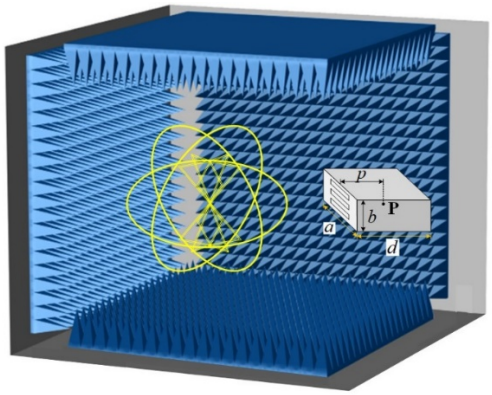

FIGURE 1. Schematic diagram of the shielding effectiveness example for a metal box.

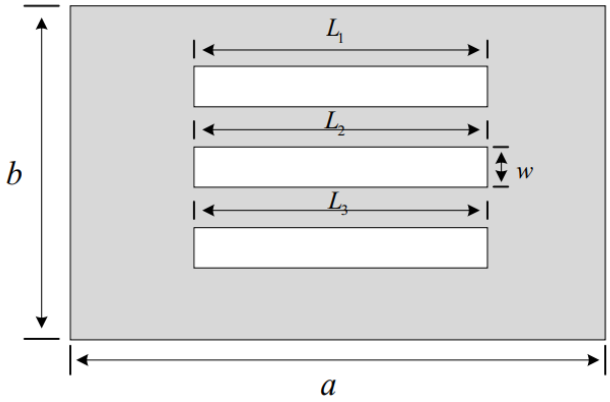

FIGURE 2. Schematic diagram of the holes of the three-hole metal box.

enhances the accuracy and stability of predictions. The definition of the failure rate tolerance is provided in Equation (12).

$$\psi_f = \left|\hat{P}_f - \bar{P}_f\right| \tag{12}$$

Similar to the steps outlined above for variance-based convergence determination, surrogate models are constructed using the training set $\{\mathbf{x}_i, y_i\}_{i=1}^{N}$. The failure rate $\hat{P}_f$ is calculated from the predicted values of the surrogate model, and the tolerance ψ_f between $\hat{P}_f$ and the reference failure rate $\bar{P}_f$ is computed. If the tolerance ψ_f is greater than the standard tolerance $\tilde{\psi}_f$, the number of training sample points N is increased by the step size d, i.e., $N = N + d$. If the tolerance ψ_f is less than or equal to the standard tolerance $\tilde{\psi}_f$, and the tolerance ψ_f for the next three step sizes remains less than or equal to $\tilde{\psi}_f$, convergence is considered to have occurred. Algorithm 2 is a code writing procedure for convergence determination based on failure rate.

It is critical to note that selecting appropriate values for standard tolerance, step size d, and the number of initial sampling points must align with the specific requirements of the engineering application. Smaller standard tolerance and step size imply higher accuracy, but slower convergence and lower computational efficiency. This configuration is particularly advantageous in scenarios characterized by low uncertainty, or when high-precision results are paramount. Conversely, in cases with substantial uncertainties, increasing the standard tolerance and step size d becomes essential to maintaining acceptable convergence speeds. Nevertheless, if the demand for accuracy is extremely high, computational efficiency can be chosen to be sacrificed. The choice of the number of initial sampling points is based on the complexity of the problem, and the more complex the problem is, the more the number of initial sampling points is.

This paper proposes two convergence determination methods, based on variance and failure rate, to evaluate the convergence of surrogate model-based uncertainty analysis from the perspectives of overall reliability and system failure, respectively. In Section 4, the convergence of three surrogate models — PCE, Kriging, and SVR — is analyzed using the metal box shielding effectiveness example.

4. APPLICATION EXAMPLE

Metal boxes are commonly used to shield electromagnetic radiation, and their surfaces typically require holes for power line pass-through and heat dissipation. However, the size of these holes can vary due to manufacturing tolerances, introducing randomness [15].

In this paper, the three-hole metal box model from [14] is used, as shown in Fig. 1. It is assumed that the lengths L_1, L_2, and L_3 of the three holes in Fig. 2 are the uncertainty factors for this example.

L_1, L_2, and L_3 are described by the following random variables:

$$\begin{cases} L_1 = 100 \times (1 + 0.1 \times \xi_1)\ [\text{mm}] \\ L_2 = 100 \times (1 + 0.1 \times \xi_2)\ [\text{mm}] \\ L_3 = 100 \times (1 + 0.1 \times \xi_3)\ [\text{mm}] \end{cases} \tag{13}$$

where ξ_1, ξ_2, and ξ_3 are uniformly distributed random variables in the interval $[-1, 1]$.

Assume that the frequency $f = 40\,\text{MHz}$. The value of the electric field strength at point **P** in the absence of a metal box is calculated as E_0. The value of the electric field strength at point **P** in the presence of a metal box is calculated as E_1. The results of the shielding effectiveness at this frequency are shown below:

$$S_E = 20 \times \log_{10}\left(\frac{E_0}{E_1}\right)\ [\text{dB}] \tag{14}$$

MCM is widely used as a reference in EMC uncertainty analysis. In this paper, the uncertainty analysis results of MCM are used as standard data, with 5000 EMC simulations performed at a large number of sampling points $\mathbf{S}_1$. The training sample points $\mathbf{S}_2$ for the three surrogate models — PCE, Kriging, and

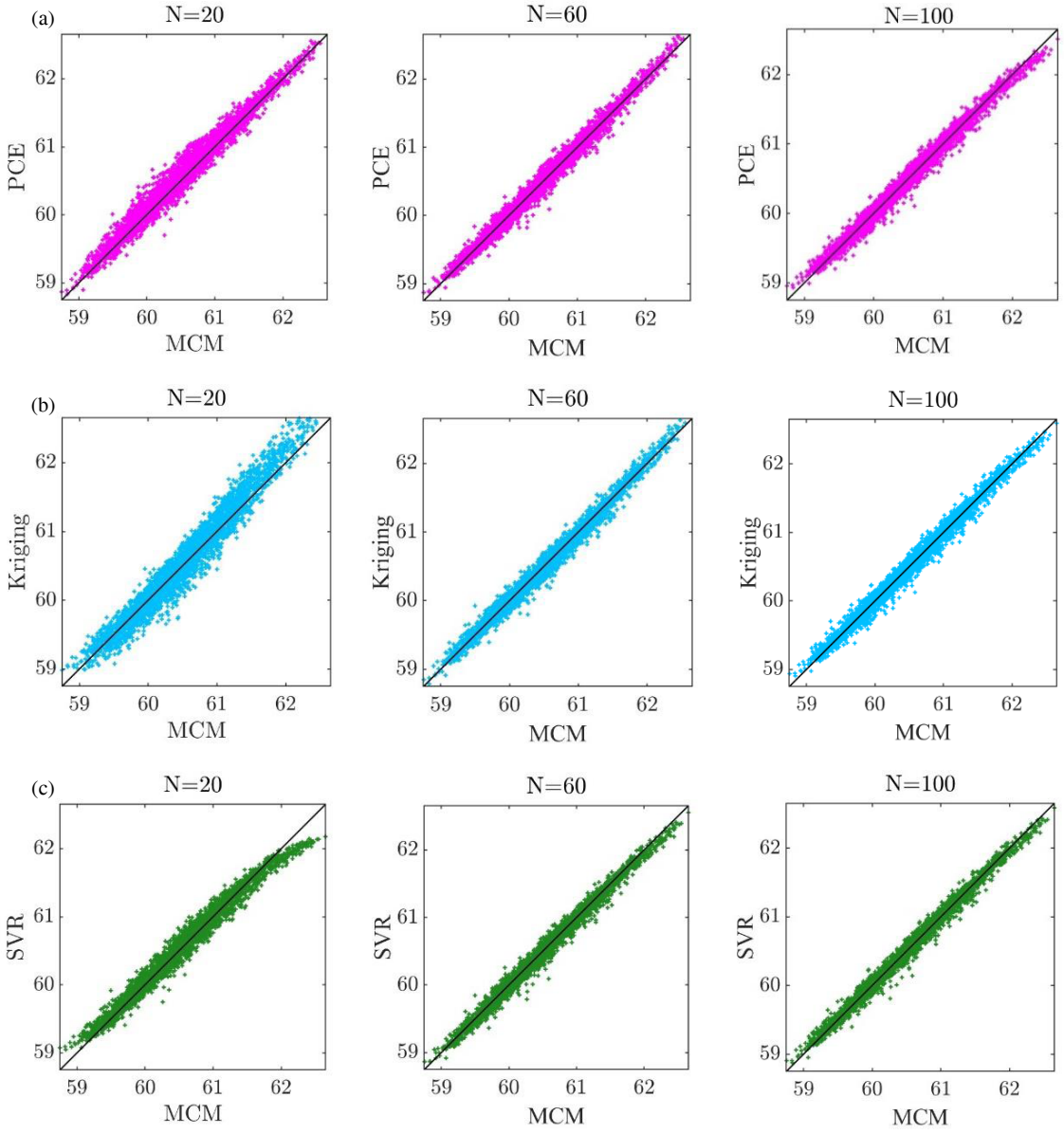

FIGURE 3. Scatter plots comparing the results (shielding effectiveness [dB]) of the three surrogate models with those of MCM. (a) Comparison of PCE and MCM simulation results. (b) Comparison of Kriging and MCM simulation results. (c) Comparison of SVR and MCM simulation results.

SVR — comprise N distinct sampling points. EMC simulations are conducted on the sample points to generate the training set $\{\mathbf{x}_i, y_i\}_{i=1}^{N}$, which subsequently facilitates the construction of the surrogate model $\hat{y} = \mathrm{M}(\mathbf{x})$. Ultimately, the results of the uncertainty analysis are derived. Fig. 3 presents scatter plots that compare the results of the three surrogate models with those of the MCM, considering varying numbers of training sample points (N = 20, 60, 100). As the number of training sample points N increases, the accuracy of the surrogate models improves. However, the scatter plots do not allow for the precise determination of the N value at which the surrogate model converges. To assess the convergence of the surrogate model, this section will employ two methods: variance and failure rate, for convergence determination.

4.1. Application of Variance-Based Convergence Determination Method to Uncertainty Analysis

Figure 4 presents the shielding effectiveness variance derived from the three surrogate models: PCE, Kriging, and SVR. As depicted in Fig. 4, the step size for the number of sampling points in this example is $d = 10$. The standard tolerance $\tilde{\psi} = 5\% \times \bar{\sigma}^2$, which is the 5% tolerance band in the figure. As illustrated in Fig. 4, all three surrogate models converge at $N = 30$ (In the three subsequent steps $N = 40$, $N = 50$, and $N = 60$, the convergence condition $\psi_v \leq \tilde{\psi}$ is satisfied). From a global standpoint, PCE, Kriging, and SVR converge simultaneously.

In order to further verify the accuracy of the proposed convergence determination method, probability density curves and Mean Equivalent Area Method (MEAM) are applied here.

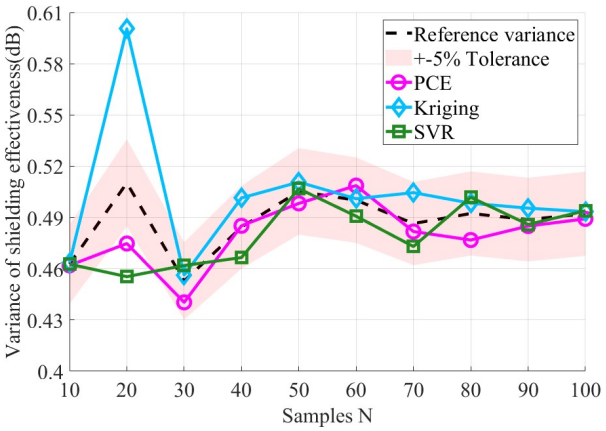

FIGURE 4. Variance convergence of shielding effectiveness.

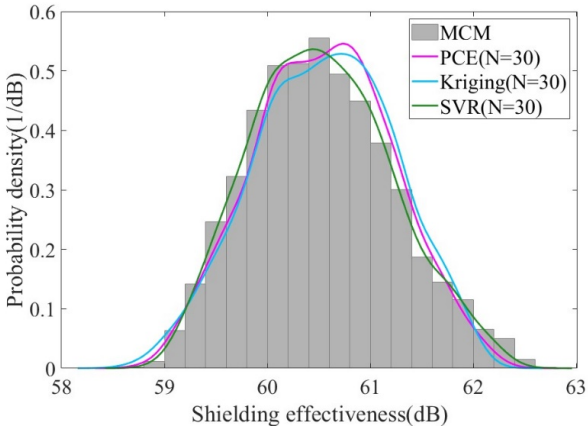

FIGURE 5. Probability density of shielding effectiveness.

Fig. 5 shows the probability density curves of MCM and the three surrogate models when they reach convergence. It can be seen that PCE, Kriging, and SVR are accurate after reaching convergence.

The MEAM assessment yields a value ranging from 0 to 1. As the value approaches 1, the difference diminishes, and the accuracy of the uncertainty analysis results improves [16]. The MEAM results for the three surrogate models are presented in Table 1. The MEAM values for all three methods exceed 0.9, with both Kriging and SVR surpassing 0.95. All three surrogate models demonstrate high accuracy in their uncertainty analysis results. Consequently, the surrogate models that converge based on variance-based convergence determination exhibit high accuracy.

TABLE 1. MEAM result.

	MEAM
PCE (N = 30)	0.9384
Kriging (N = 30)	0.9553
SVR (N = 30)	0.9611

The variance-based convergence determination proposed in this paper is compared here with the improved MEAM-based convergence determination method proposed in [9]. Both methods judge convergence from the perspective of global performance. The idea of convergence determination in [9] is as follows: the initial number of sample points is selected as N, and the step size is $2N$. The surrogate model is constructed based on N and $2N$ sample points respectively, and the MEAM values of the two surrogate models before and after are calculated. If the MEAM value is greater than 0.95, it is determined that $2N$ is the number of sample points where the surrogate model converges. Table 2 shows the convergence determination process of applying this method in the example of this paper. The initial number of sample points is consistent with the variance-based convergence determination method.

The improved MEAM convergence determination method is applied to determine the convergence of PCE, Kriging, and SVR. SVR converges only at $N = 20$, PCE reaches convergence at $N = 40$, while Kriging reaches convergence at $N = 80$. This shows the lack of generalizability and flexibility of this method. Although SVR reaches convergence at a faster rate with the determination of this method (compared to the variance-based convergence determination proposed in this paper), PCE and Kriging converge at a slower rate. Kriging, which reaches convergence only at $N = 80$ in the improved MEAM determination method, is a great waste of computational resources. The improved MEAM convergence determination method does not apply to Kriging. The variance-based convergence determination method proposed in this paper is able to integrate the properties of multiple surrogate models, a property that makes it generalizable better than the improved MEAM. In terms of flexibility, the improved MEAM chooses a step size of $2N$. This feature can lead to a step size so large when the initial number of sample points is large that it can waste computational resources and reduce efficiency.

4.2. Application of Failurerate-Based Convergence Determination Methods to Uncertainty Analysis

Various applications impose distinct requirements on the shielding effectiveness of metal enclosures. In this paper, as referenced in [17], it is assumed that the shielding enclosure under consideration is a "general" electromagnetic shielding box, with shielding index requirements of $S_E > 60\,[\mathrm{dB}]$. Hence, the failure domain for the shielding effectiveness of the metal enclosure is as follows:

$$F = \{\mathbf{x} : S_E(\mathbf{x}) < 60\,[\mathrm{dB}]\} \tag{15}$$

The failure rate of shielding effectiveness, derived from the three surrogate models — PCE, Kriging, and SVR — is presented in Fig. 6. The step size for the number of sampling points is $d = 10$. The standard tolerance is $\tilde{\psi}_f = 5\% \times \bar{P}_f$, corresponding to the 5% tolerance band in the figure. As depicted in the figure, PCE converges at $N = 50$. SVR achieves convergence at $N = 40$. In contrast, Kriging converges only at $N = 30$. Therefore, from the perspective of system failure, Kriging can reach convergence at a faster rate.

To further validate the accuracy of the proposed convergence determination method, both the probability density curves and the relative errors of the failure rates are utilized. As observed from the probability density curves of MCM and the three sur-

TABLE 2. Convergence determination process based on improved MEAM.

	N = 10 and N = 20	N = 20 and N = 40	N = 40 and N = 80
PCE	0.9463	0.9681	0.9838
Kriging	0.8786	0.8988	0.9867
SVR	0.9921	0.9852	0.9642

TABLE 3. Failure rate and relative error.

	failure rate	relative error
MCM	24.39%	/
PCE (N = 50)	25.18%	3.24%
Kriging (N = 30)	21.49%	11.89%
SVR (N = 40)	24.41%	0.08%

TABLE 4. Comparison of simulation time.

	t_{EMC}	t_{modle}
MCM	360.83 h	/
PCE (N = 50)	3.61 h	3.5 s
Kriging (N = 30)	2.17 h	7.5 s
SVR (N = 40)	2.89 h	5.3 s

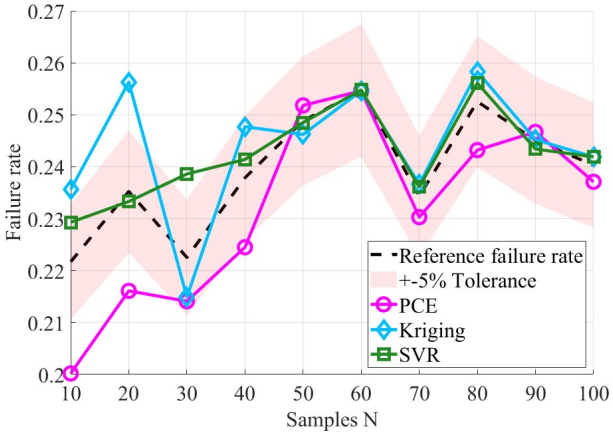

FIGURE 6. Failure rate convergence of shielding effectiveness.

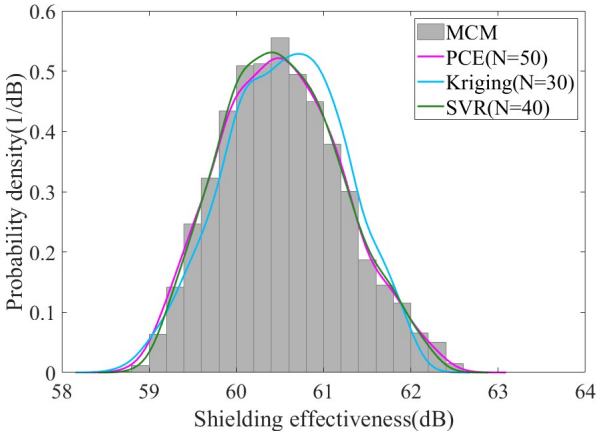

FIGURE 7. Probability density of shielding effectiveness.

rogate models at convergence in Fig. 7, PCE, Kriging, and SVR exhibit high accuracy upon convergence.

The shielding effectiveness failure rate results for the four uncertainty analysis methods including MCM are shown in Table 3. The failure rate P_f of MCM is 24.39%, which is used as a criterion. The relative errors in the failure rates of PCE and SVR are minimal, suggesting that their results closely match those of MCM. The relative error in Kriging's failure rate is slightly higher than that of PCE and SVR; however, its results still fall within the high accuracy range. Therefore, the convergence determination based on failure rate can precisely identify the number of sample points needed for each surrogate model to achieve convergence from the system failure perspective. This approach ensures that the constructed surrogate models exhibit high accuracy.

Finally, the computational efficiencies of MCM and the three converged surrogate models are compared. A single EMC simulation takes 4.33 minutes, while running 5000 MCM simulations requires 360.83 hours. PCE achieves convergence after 50 EMC simulations, requiring a total of 3.61 hours. SVR reaches convergence after 40 simulations, taking 2.89 hours. Kriging attains convergence with just 30 simulations, requiring only 2.17 hours. The computational cost of surrogate model predictions is negligible compared to that of EMC simulations. The computational time required for each method is summarized in Table 4. The surrogate model-based uncertainty analysis method demonstrates a significant efficiency advantage over MCM.

5. CONCLUSION

To address the gap in convergence determination within surrogate model-based uncertainty analysis, this paper introduces two convergence determination methods based on variance and failure rate. By integrating the variance or failure rate of the PCE, Kriging, and SVR models as reference standards, the issues of overfitting and underfitting associated with individual models are effectively mitigated (e.g., the relative error in the failure rate of SVR at $N = 40$ is only 0.08%), thereby enhancing the robustness of the convergence determination. The two convergence determination methods can be used to determine the convergence of the surrogate model from the perspectives of global and system failure, respectively. The variance-based strategy pays more attention to global performance, while the failure rate-based strategy pays more attention to the system failure risk. This paper breaks through the limitation of

the traditional single evaluation index and provides a flexible selection basis for different engineering requirements (system stability priority vs. fail-safe priority). Finally, the practicality and reliability of the two proposed convergence determination methods are verified by analyzing the uncertainty of the three surrogate models in the metal box shielding effectiveness example.

ACKNOWLEDGEMENT

This paper is supported by "the Open Fund of National Center for International Research of Subsea Engineering Technology and Equipment" (Project No. HG20240201).

REFERENCES

[1] Bai, J., S. Huo, A. Duffy, and B. Hu, "Improvement of nonembedded EMC uncertainty analysis methods based on data fusion technique," *IEEE Transactions on Electromagnetic Compatibility*, Vol. 66, No. 6, 1999–2009, Dec. 2024.

[2] Tan, T., T. Jiang, Y. Wu, Y. Zhu, and Y. Chi, "Safety assessment of gender-specific human electromagnetic exposure with aortic valve stents for EV-WPT," *Applied Computational Electromagnetics Society Journal (ACES)*, Vol. 39, No. 08, 742–753, Aug. 2024.

[3] Lagouanelle, P., F. Freschi, and L. Pichon, "Adaptive sampling for fast and accurate metamodel-based sensitivity analysis of complex electromagnetic problems," *IEEE Transactions on Electromagnetic Compatibility*, Vol. 65, No. 6, 1820–1828, Dec. 2023.

[4] Huo, S., Y. Song, Q. Liu, and J. Bai, "Improving kriging surrogate model for EMC uncertainty analysis using LSSVR," *Applied Computational Electromagnetics Society Journal (ACES)*, Vol. 39, No. 07, 614–622, Jul. 2024.

[5] Lagouanelle, P., V.-L. Krauth, and L. Pichon, "Uncertainty quantification in the assessment of human exposure near wireless power transfer systems in automotive applications," in *2019 AEIT International Conference of Electrical and Electronic Technologies for Automotive (AEIT AUTOMOTIVE)*, 1–5, Turin, Italy, Jul. 2019.

[6] Wang, T., Q. Yu, B. Li, G. Lv, Y. Wu, and S. Guan, "Uncertainty quantification of human electromagnetic exposure from electric vehicle wireless power transfer system," *IEEE Transactions on Intelligent Transportation Systems*, Vol. 24, No. 8, 8886–8896, Aug. 2023.

[7] Trinchero, R., M. Larbi, H. M. Torun, F. G. Canavero, and M. Swaminathan, "Machine learning and uncertainty quantification for surrogate models of integrated devices with a large number of parameters," *IEEE Access*, Vol. 7, 4056–4066, 2018.

[8] Sedaghat, M., R. Trinchero, Z. H. Firouzeh, and F. G. Canavero, "Compressed machine learning-based inverse model for design optimization of microwave components," *IEEE Transactions on Microwave Theory and Techniques*, Vol. 70, No. 7, 3415–3427, Jul. 2022.

[9] Bai, J., J. Sun, and N. Wang, "Convergence determination of EMC uncertainty simulation based on the improved mean equivalent area method," *Applied Computational Electromagnetics Society Journal (ACES)*, Vol. 36, No. 11, 1446–1452, Dec. 2021.

[10] Hu, B., Y. Song, P. Wang, S. Lin, and J. Bai, "Convergence determination method for uncertainty analysis surrogate models based on MEAM," *Progress In Electromagnetics Research M*, Vol. 129, 91–97, 2024.

[11] Han, Z.-H. and S. Görtz, "Hierarchical kriging model for variable-fidelity surrogate modeling," *AIAA Journal*, Vol. 50, No. 9, 1885–1896, Sep. 2012.

[12] Klink, D. and P. Meyer, "A comparison of techniques for finding coefficients of polynomial chaos models for antenna problems," *International Journal of RF and Microwave Computer-Aided Engineering*, Vol. 31, No. 8, e22729, 2021.

[13] Samad, A., K.-Y. Kim, T. Goel, R. T. Haftka, and W. Shyy, "Multiple surrogate modeling for axial compressor blade shape optimization," *Journal of Propulsion and Power*, Vol. 24, No. 2, 301–310, Mar. 2008.

[14] Huo, S., Z. Xue, Y. Zhou, J. Yao, and J. Bai, "Credibility assessment of EMC uncertainty analysis based on failure rate," *Progress In Electromagnetics Research Letters*, Vol. 124, 55–61, 2025.

[15] Huo, S., J. Bai, H. Cao, and J. Yao, "Performance analysis of electromagnetic frequency response prediction based on LSTM," *IEEE Letters on Electromagnetic Compatibility Practice and Applications*, Vol. 6, No. 4, 126–131, Dec. 2024.

[16] Bai, J., L. Wang, D. Wang, A. P. Duffy, and G. Zhang, "Validity evaluation of the uncertain EMC simulation results," *IEEE Transactions on Electromagnetic Compatibility*, Vol. 59, No. 3, 797–804, Jun. 2017.

[17] GB/T 50719-2011, Technical code for electromagnetic shielded enclosure.